NASA Technical Memorandum 87210

Thermal Aging Effects in Refractory Metal Alloys

(NASA-TM-87210) THERMAL AGING EFFECTS IN REFRACTORY METAL ALLOYS (NASA) 28 p
HC A03/MF A01 CSCL 11F

N86-16334

Unclas
G3/26 05288

Joseph R. Stephens
Lewis Research Center
Cleveland, Ohio

Prepared for the
Third Symposium on Space Nuclear Power Systems
sponsored by The American Nuclear Society
Albuquerque, New Mexico, January 13-15, 1986

NASA

Thermal Aging Effects in Refractory Metal Alloys

Joseph R. Stephens

National Aeronautics and Space Administration

NASA Lewis Research Center

Cleveland, Ohio 44135

ABSTRACT

The alloys of niobium and tantalum are attractive from a strength and compatibility viewpoint for high operating temperatures required in materials for fuel cladding, liquid metal transfer, and heat pipe applications in space power systems that will supply from 100 kWe to multi-megawatts for advanced space systems. To meet the system requirements, operating temperatures ranging from 1100 to 1600 K have been proposed. Expected lives of these space power systems are from 7 to 10 yr. A program was conducted at NASA Lewis to determine the effects of long-term, high-temperature exposure on the microstructural stability of several commercial tantalum and niobium alloys. Variables studied in the investigation included alloy composition, pre-age annealing temperature, aging time, temperature, and environment (lithium or vacuum), welding, and hydrogen doping. Alloys were investigated by means of cryogenic bend tests and tensile tests. Results showed that the combination of tungsten and hafnium or zirconium found in commercial alloys such as T-111 and Cb-752 can lead to aging embrittlement and increased susceptibility to hydrogen embrittlement of ternary and more complex alloys. Modification of alloy composition helped to eliminate the embrittlement problem.

E-2808

INTRODUCTION

Niobium and tantalum alloys are being considered for use in advanced space-power systems in applications such as nuclear fuel-element cladding, liquid metal transfer, and heat pipes. Minimum requirements for these applications

include high creep resistance in the temperature range 1100 to 1600 K, a ductile-brittle transition temperature well below room temperature, good formability and weldability, and corrosion resistance to liquid alkali metals such as lithium, sodium, and potassium. Results have shown that severe corrosion can occur in tantalum-10 tungsten (Ta-10 W) (weight percent) contaminated with oxygen concentrated at grain boundaries, because of preferential attack of these high-oxygen content regions by liquid metals (Moss et al., 1970). Because of this potential corrosion problem a reactive element such as hafnium is added to the Ta-base alloy to serve as a getter for oxygen. The stable oxide that forms, hafnium dioxide (HfO_2), is not attacked by the alkali metal thus permitting operation of Ta-base alloys in alkali metal environments even when oxygen contamination exists. Tests have shown that T-111 (Ta-8W-2Hf) can successfully operate for several thousand hours in an alkali metal environment with little or no corrosion (Moss et al.,1970). However, room-temperature embrittlement has been noted in T-111 specimens aged for 1000 hr or longer at 1275 K. A program conducted at NASA Lewis by Watson and Stephens (1972) indicated that the brittle intergranular fractures observed in aged T-111 were caused by hydrogen embrittlement during post-aging handling operations. The results further suggested that the presence of HfO_2 at the grain boundaries of T-111 aged at 1315 K may be associated with its subsequent increased sensitivity to hydrogen embrittlement. The primary purposes of a series of studies conducted at NASA Lewis by Stephens (1974, 1975, 1975, 1977, and 1977) were to investigate in greater detail the causes of embrittlement after long term aging and to seek means of alleviating this problem through alloy modification.

A total of eight Ta-base alloys, three Nb-base alloys, and one Mo-base alloy were investigated. Test variables included pre-age annealing temperature, simulated butt welding, and aging conditions (time, temperature, and

environment). Evaluation included bend testing and tensile testing to measure effects on ductility and strength.

EXPERIMENTAL

Materials

The chemical compositions of the alloys evaluated in this study are listed in Table 1. The alloys were obtained in the form of sheet ranging in thickness from 0.75 to 1.5 mm thick and in the form of tubing having a 19 mm o.d. and a 1.5 mm wall thickness. To evaluate the effect of welding, a gas-tungsten-arc bead-on-plate weld (to simulate a butt weld) was made along the longitudinal centerline of some of the Ta-base alloy specimens. A standard annealing treatment for the Ta-base alloys consisted of 1 h at 1925 K plus 1 h at 1590 K. Some specimens were also annealed at 2090 and 2250 K instead of the 1925 K standard heat treatment. Resulting grain sizes of 26, 52, and 150 μm were achieved for annealing temperatures of 1925, 2090, and 2255 K, respectively. Niobium alloys were annealed at 1620 K for 1 h while the Mo-base alloy was annealed at 1700 K for 1 h.

Aging

Tantalum alloys were aged at 1315 K for 1000 and 5000 h in vacuum and at 1200 and 1425 K for 1000 h in both vacuum and a lithium environment. Niobium and Mo alloys were annealed only in vacuum for 1000 h at temperatures ranging from 975 to 1300 K.

Hydrogen Doping

Hydrogen doping was accomplished by heating several specimens from each alloy in an evacuated furnace to 1315 K (Ta alloys) and 1100 K (Nb and Mo alloys), at which point hydrogen was introduced into the furnace to a pressure of 13 kN/m^2. The specimens were held at temperature for 10 minutes followed by cooling in a helium atmosphere.

Evaluation

Bend and tensile testing were used as the primary measurement to determine the effects of aging, alloy composition, and other variables on the mechanical properties of the three alloy systems. Light and electron microscopy along with chemical analyses were used to further characterize the alloys.

RESULTS

At the time these programs were conducted, in the early 1970's, emphasis was primarily on tantalum-base alloys and niobium-base alloys. Only a minor interest in the molybdenum-base alloys as candidate space power system materials existed due to the fabricability problems associated with forming heat pipes, fuel cladding configurations, and so on. Because of this emphasis, our work focused primarily on the Ta-base alloy T-111, while secondarily, niobium alloys were studied because of their similarity to Ta-base alloys. It was desirable to determine if the aging embrittlement problem noted in some instances for the Ta alloys also occurred in Nb alloys and under similar conditions. Molybdenum alloys were investigated to include a Group VI alloy with the Group V alloys, Ta and Nb. The results will be discussed in the order of emphasis at the time the research was conducted. Included among the Nb alloys was Nb-1Zr which is the primary alloy under consideration for current space power systems such as the SP-100 Program.

Tantalum-Base Alloys

Chemical analysis

Interstial impurities were determined for the alloys before and after aging. Results indicated that aging in lithium or vacuum had no apparent effect on the nitrogen content of the Ta alloys. In contrast, the oxygen data revealed that aging in lithium substantially reduced the oxygen content of the Ta alloys at 1315 and 1425 K (for example from 65 to 33 ppm and from 33 to 8 ppm in other cases), and to a lesser extent at 1200 K (from 65 to 44 ppm).

Aging in vacuum did not reduce the oxygen content of the alloys except for T-111 which had been pre-aged annealed at 2090 and 2255 K (to 52 and 34 ppm). The hydrogen analysis for doped specimens revealed a pickup of about 5 to 10 ppm hydrogen for all the alloys in the pre-age annealed condition and from 10 to 30 ppm hydrogen for aged specimens.

Bend ductility

The effect of pre-age annealing temperature on the ductility of T-111 tube that was subsequently aged in lithium for 1000 h at 1315 K is shown in Figure 1. Specimens were brittle at 77 K after all pre-age annealing treatments and, as the pre-age annealing temperature was increased to 2255 K, T-111 became brittle at room temperature. This is attributed in part to the large (150 μm) grain size of these specimens compared with the grain size of 26 and 52 μm for specimens annealed at 1925 and 2090 K, respectively. Figure 2 illustrates the effects of aging temperature on the bend ductility of T-111 tube. It is shown that the annealed specimens and those aged at 1200 and 1425 K could undergo a full 180°, 0t bend at 77 K without fracture or cracking while specimens aged at 1315 K fractured with essentially no ductility. This lack of ductility will be termed aging embrittlement and seems to be confined to specimens aged over a narrow temperature range near 1315 K. The remaining aging conditions investigated (time and environment) had very little effect on the bend ductility of T-111. Extending the aging time to 5000 h at 1315 K resulted in brittle behavior at 77 K and ductile behavior at room temperature, results similar to those obtained after the standard 1000 h treatment.

Several of the sheet bend specimens were welded before the standard aging treatment and in the as welded condition were ductile at 77 K. Since the standard aging treatment produced embrittlement at 77 K, bend tests on welded and aged T-111 were conducted only at room temperature where all specimens which had been both welded and aged were brittle. A similar finding was reported

previously for welded T-111 after aging for 1000 to 10 000 hr over the temperature range 1255-1425 K (Lessmann and Gold 1970). The large grain size developed in the weld area is assumed to contribute to the embrittlement. Bend test results are summarized in Figure 3 for T-111 sheet doped with hydrogen. It should be noted that sheet aged at 1200 K and then doped with 10 ppm hydrogen still exhibited some ductility at 77 K. In contrast, T-111 sheet aged at 1315 and 1425 K and then doped with 10 ppm hydrogen was brittle at the less severe test temperature of 300 K. This corresponds to an increase of over 200 K in the ductile-brittle transition temperature (DBTT) of T-111 sheet and is in agreement with previous results reported by Watson and Stephens (1972). Similar results were found on tubing material also. However this embrittlement is not solely related to the bulk hydrogen content of 10 ppm since varying degrees of ductility were observed depending on aging conditions.

The effects of alloy composition are most interesting and give some insight into the reasons for aging embrittlement and susceptibility to hydrogen embrittlement in Ta-base alloys. All compositions were ductile at 77 K in the pre-age annealed condition. Only two of the alloys, Ta-8W-2Hf (T-111) and Ta-8W-3Hf, were susceptible to aging embrittlement. These two alloys contain the greatest amount of W and Hf, suggesting that the combined levels of W and Hf have an important effect on the alloy's susceptibility to aging embrittlement. Bend data for hydrogen-doped Ta alloys are shown in Figure 4. In the annealed condition only T-111 indicated any evidence of loss in ductility at 77 K owing to the addition of approximately 8 ppm hydrogen. Aging and then doping with hydrogen resulted in embrittlement of all the alloys except the two binary alloys: Ta-10W exhibited only slight surface cracks after a 180° bend at 77 K and Ta-2Hf showed no loss of ductility at 77 K. Hydrogen embrittlement was most severe in the Ta-8W-2Hf (T-111) and Ta-8W-3Hf alloys, the specimens being brittle at 300 K after aging either in lithium or vacuum.

In contrast, the ductility at 300 K of the remaining ternary alloys and ASTAR-811C showed a dependence on aging environment which in turn could be related to the hydrogen content of the specimens, 12 ppm for vacuum aging and 25 ppm for lithium aging. The reduced oxygen content after lithium aging is believed to have permitted higher amounts of hydrogen to enter the specimens during subsequent hydrogen doping.

Tensile properties

The tensile behavior of the Ta alloys was similar and was characterized by three distinct types of stress-strain curves depending on the test temperature, as shown in Figure 5. At lower test temperatures (from 300 to 895 K) the alloys exhibited a yield point drop that is attributed to the locking of dislocations by interstial impurities present in the alloys. At the highest test temperatures (1315 to 1455 K) smooth stress-strain curves were observed, while at the intermediate test temperatures (primarily from 1035 to 1315 K) serrated flow curves characterized the alloys. This behavior is attributed to dynamic strain aging, which is due to repeated breaking away of dislocations by impurity atmospheres and to subsequent locking of dislocations by impurity atmospheres. Oxygen has previously been identified by Sheffler et al. (1970) to be the responsible species.

Based on a comparison of the data for sheet and tubing, it is concluded that processing history does not have a significant effect on the tensile properties of T-111. The effects of aging time and environment on the tensile properties of T-111 sheet are shown in Figure 6. It may be seen that the various conditions had little effect on the yield strength and only a minor effect on ultimate tensile strength. Over the temperature range of about 875 to 1425 K the ultimate tensile strength was lowered by minimizing dynamic strain aging.

The effect of aging on the tensile strength of each of the other alloys is shown in Figure 7. It should be noted that both the ultimate and yield strength of Ta-10W decreased substantially, with lithium having a greater effect than vacuum. Aging of Ta-2Hf minimized the effects of dynamic strainage strengthening over the 875 to 1315 K temperature range for the ultimate tensile strength and decreased the yield strength primarily over the 300 to 775 K temperature range. In contrast, the remaining ternary alloys exhibited only minor variations in strength with aging conditions.

Scanning electron microscopy

Figure 8 shows scanning electron micrographs of fractured surfaces of the eight Ta alloys that had been aged, hydrogen-doped, and then bend tested at 300 K. It should be noted that Ta-10W (Figure 8(a)) failed in a ductile manner (fracture achieved by repeated bending in opposite directions) and was free of precipitate particles at grain boundaries. With increasing Hf content in the Ta-8W base alloys, brittle intergranular fracture dominates the microstructure with some evidence of ductile tearing, as shown in Figures 8(b) to (d) for Hf levels of 0.5, 0.7, and 1.0, respectively. Alloys with larger Hf additions (2.0 and 3.0 percent) fractured in a completely brittle manner as shown in Figures 8(e) and (f). Brittle intergranular failure also characterized the Ta-4W-2Hf alloy (Figure 8(g)). However, on complete removal of W from the alloy system, ductile failure characterized the Ta-2Hf alloy (Figure 8(h)), and the grain boundaries were free of precipitate particles, as were those of Ta-10W. Precipitate particles were observed in all the ternary alloys and in ASTAR-811C, which exhibited either predominantly or totally intergranular failure. The Ta-8W-3Hf alloy contained the greatest concentration of precipitate particles at the grain boundaries. As either the Hf content is reduced to 0.5 to 1.0 percent or the W is reduced to 4 percent, fewer particles were observed at the grain boundaries. It is this variation in amount of

precipitates at the grain boundaries that is believed to account for the aging embrittlement exhibited only by the Ta-8W-2Hf and Ta-8W-3Hf alloys. The remaining ternary alloys and ASTAR-811C with fewer precipitates at the boundaries and the two binary alloys with an absence of precipitate particles did not exhibit aging embrittlement. Upon doping with hydrogen, all the alloys with particles at the grain boundaries exhibited hydrogen embrittlement. The identity of the particles was achieved by performing characteristic x-ray analysis in the scanning electron microscope using an energy dispersive spectrometer. Figure 9(a) shows the fracture surface of a sheet T-111 specimen at 1315 K. Analysis of the grain boundary surface away from the particles is shown in Figure 9(b) while Figures 9(c) and (d) show analyses of particles A and B in Figure 9(a) located at a grain boundary intersection and on the grain boundary surface, respectively. The analysis demonstrates that the particles are Hf rich. In addition, by using a step scan technique oxygen peaks were observed at grain boundaries corresponding to Hf peaks. Based on these results it is concluded that the particles are HfO_2. The results suggest that not only is composition of the Ta-base alloys important to the aging embrittlement problem, but aging temperature is of extreme importance as well. The results suggest that a critical temperature for Ta-base alloys is over the range 0.35 to 0.47 T_m on a homologous temperature basis.

Niobium-Base Alloys

As mentioned previously, primary emphasis was placed on Ta-base alloys because of their high priority at the time of these investigations. After analyzing the aging results obtained on the Ta alloys, a similar study was conducted on three Nb-base alloys. Alloys included were C-103 and Nb-1Zr, both of interest for space power systems. In addition, Cb-752 was selected because of its composition. The combination of W and Zr in this alloy suggested that aging embrittlement would also occur in this alloy and thus would

provide an opportunity to determine how widespread the aging embrittlement phenomenon is in refractory metal alloys. Nb-base alloys were evaluated by chemical analysis, bend tests, and metallography.

Chemical analysis

Aging of the Nb-base alloys was conducted in vacuum only and chemical analyses before and after aging indicated no significant changes in interstial content of the alloys. Hydrogen doping was achieved in a manner similar to that used for the Ta alloys except that a temperature of 1100 K was used for the Nb alloys which on a homologous temperature basis is equivalent to that used for the Ta alloys. After doping, hydrogen contents of the alloys were about 60, 50, and 40 ppm for C-103, Nb-1Zr, and Cb-752, respectively.

Bend ductility

Bend tests were conducted on specimens in the annealed condition and after aging for 1000 h at temperatures ranging from 975 to 1300 K. A comparison of the bend test results is shown in Figure 10. It should be noted in Figures 10(a) and (b) that the bend ductilities for C-103 an Nb-1Zr are not imparied as a result of aging over the critical temperature range 0.35 to 0.47 T_m. In contrast, for Cb-752, Figure 10(c), aging at 1175 K (0.43 T_m) resulted in a ductile-brittle transition temperature of 125 K, an increase of at least 50 K. Thus aging embrittlement occurs in Cb-752 in a manner quite similar to the behavior observed in Ta-base alloys such as T-111.

A comparison of the effects of hydrogen doping on the ductility of the Nb alloys is shown in Figure 11. Hydrogen doping to an average content of 60 ppm in C-103 did not affect the ductility at 77 K, Figure 11(a) for the annealed or aged conditions. The DBTT of the annealed Nb-1Zr alloy was below 77 K after doping to about 50 ppm hydrogen. In contrast, the DBTT of all aged and hydrogen-doped Nb-1Zr specimens was 175 K, as illustrated in Figure 11(b). A general trend noted is that ductility at 77 and 125 K increases with increasing aging

temperature which may be attributed to a change in microstructure observed in these alloys. Aging at 975 and 1100 K produced platelet-type particles primarily at grain boundaries and after aging at 1200 K these particles were primarily intergranular. In contrast, aging at the higher temperatures of 1250 and 1300 K, the microstructures of Nb-1Zr were free of precipitate particles. The presence of the precipitate particles combined with hydrogen may account for the low ductility for specimens aged at lower temperatures. Ductility increased for higher aging temperatures, which also resulted in the disappearance of the platelet particles. The effect of hydrogen doping on the DBTT of Cb-752 is illustrated in Figure 11(c). Hydrogen doping to an average level of 40 ppm increased the DBTT of annealed Cb-752 to above room temperature, 325 K. The highest DBTT was for specimens aged at the intermediate temperature of 1175 K, the temperature where aging embrittlement occurred in Cb-752.

Scanning electron microscopy

Since aging embrittlement occurred in the Cb-752 alloy, results for this alloy only will be presented here. The fracture surface of a Cb-752 specimen aged at 1175 K and subsequently tested at 77 K is shown in Figure 12. Aging embrittlement which occurred at this temperature produced a brittle, intergranular fracture. Particles are observed on the grain boundary surfaces and at grain boundary intersections. Analysis of a grain-boundary surface area free of particles is shown in Figure 12(b). Only Nb and W were detected in this area. In contrast, analysis of a grain-boundary region containing a precipitate particle exhibited peaks for Zr in addition to the Nb and W peaks shown in Figure 12(c). As postulated, Zr-rich particles formed at grain boundaries in Cb-752 in a manner similar to the Hf-rich particles formed in the Ta alloys.

Molybdenum-Base Alloy, Mo-TZM

Since their is some interest in Mo-base alloys for space power systems, the commercial alloy Mo-TZM was chosen to round out the study of hydrogen embrittlement of refractory metal alloys. It is well known that hydrogen has a very low solubility in Group VI alloys such as Mo and also the reactive metal (Zr and Ti) content in Mo-TZM is very low so that aging embrittlement and increased susceptibility to hydrogen was not predicted for this Mo-base alloy.

Chemical analysis

As with the Nb alloys, Mo-TZM was aged only in vacuum. No change in interstitial content resulted from the 1000 h aging and no increase in hydrogen content was detected upon subsequent doping attempts. Hydrogen content after all the aging treatments was near 1 ppm.

Bend ductility

Bend DBTT results are shown in Figure 13 for Mo-TZM in the aged condition. In the annealed condition the DBTT was 260 K. Aging at 975, 1100, and 1200 K resulted in a DBTT of 260 K while aging at 1250 and 1300 K produced a slight increase in the DBTT to 275 K. This increase in DBTT is believed to be due to a change in carbide morphology rather than aging embrittlement as was observed in the Ta and Nb alloys. The DBTTs after hydrogen doping were similar to those in the aged condition which was expected since hydrogen content did not increase during doping.

Scanning electron microscopy

Scanning electron microscopy results for a Mo-TZM specimen tested at 260 K after aging at 1250 K are shown in Figure 14. The fracture appearance for this specimen (60° bend angle) reveals a mixed mode of failure involving areas of ductile tearing, transgrannular cleavage, and grain-boundary fracture. Only Mo was detected in this specimen at the grain-boundary fracture area.

DISCUSSION

The aging and hydrogen embrittlement of T-111 and other similar Ta base alloys is believed to be due to Hf segregation at grain boundaries. The absence of particle formation in Ta-2Hf suggests that the presence of W in the ternary alloys affects the rate and degree of Hf segregation that is observed in these alloys. This may occur due to the lattice contraction that occurs upon adding W to Ta (Pearson 1974) causing the larger Hf atom to segregate to misfit or grain boundary areas. Competing with this equilibrium segregation process is diffusion which will tend to evenly disperse the solute at higher temperatures (Mc Lean 1957). Hence, T-111 aged at 1590K did not exhibit precipitate particles. Also, this material did not exhibit aging embrittlement and was not susceptible to hydrogen embrittlement.

The results for the Nb alloys indicate a similar type behavior as was observed for the Ta alloys. Segregation did not occur in the binary Nb-1Zr alloy, which would be expected to behave similarly to the Ta-2Hf alloy. In addition, Hf segregation did not occur in the C-103 alloy with 10 percent Hf. However, in Cb-752, which contains both W and Zr, grain-boundary Zr segregation occurred and produced about a 50 K increase in the DBTT of this alloy. Aging at a critical temperature of 0.41 to $0.43T_m$ in these alloys produces the aging embrittlement. Aging at higher temperatures resulted in ductile behavior as did aging at lower temperatures. Homogenization by diffusion apparently occurs at the higher temperatures while longer times at the lower temperature will result in the aging embrittlement phenomenon occurring due to Hf or Zr segregation, since longer times are required for lower diffusion rates. The results for Cb-752 are best compared with the Ta-4W-2Hf alloy. On an atom percent basis, Cb-752 contains 5.2 W to 2.9 Zr. Therefore, with aging temperatures based on a homologous temperature scale and compositions expressed on an atom basis, results indicate that the Ta-base and Nb-base alloy systems can be

described by the same mechanisms. Although the alloying elements Ti and Zr in Mo have larger atomic radii than does Mo and would be expected to segregate at grain boundaries during long term aging, this phenomenon was not observed in Mo-TZM. Consequently, aging embrittlement did not occur in this alloy. The low concentrations of the reactive elements and the carbon content of Mo-TZM may account for this behavior. The reactive elements were present as carbides or in solution at these low levels.

APPLICATION OF RESULTS

The studies described herein have established that aging embrittlement is most pronounced as a result of long term aging near 0.41 to 0.43 T_m (but can occur over the temperature range 0.35 to 0.47 T_m) in alloys with 4 to 8 atomic percent W and 2 to 3 atomic percent Hf or Zr. If the use of alloys with combinations of solutes in this concentration range is proposed for the critical temperature range, then extreme care should be taken during subsequent handling or maintenance after cool down to room temperature. Great care should also be exercised to prevent exposure to hydrogen.

CONCLUSIONS

Based on a study of the long term aging effects and susceptibility to hydrogen embrittlement of Ta, Nb, and Mo alloys the following conclusions are drawn:

1. Aging embrittlement occurs in Ta and Nb alloys that contain a critical combination of W (4 to 8 atomic percent) and Hf or Zr (2 to 3 atomic percent) that have been aged for 1000 to 10 000 h in the homologous temperature range of 0.35 to 0.47 T_m.

2. Alloys exhibiting aging embrittlement are much more susceptible to hydrogen embrittlement as evidenced by a further increase in the ductile-brittle transition temperature of these alloys.

3. Scanning electron microscopy demonstrated that segregation of Hf and Zr to grain boundaries led to aging embrittlement and increased susceptibility to hydrogen embrittlement in these alloys.

4. The Mo-base alloy Mo-TZM did not experience aging or hydrogen embrittlement as a result of long term aging over a similar homologous temperature range.

ACKNOWLEDGEMENTS

This work was conducted at the NASA Lewis Research Center. The helpful discussions with Gordon K. Watson and Robert H. Titran are greatly appreciated.

REFERENCES

G.G. Lessman, and R.E. Gold, "Determination of the Weldability and Elevated Temperature Stability of Refractory Metal Alloys. II - Long-Time Temperature Stability of Refractory Metal Alloys," NASA CR-1608, (1970).

D. McLean, Grain Boundaries in Metals, Clarendon Press, Oxford (1957).

T.A. Moss, R.L. Davies, and G.J. Barna, "Refractory-Alloy Requirements for Space Power Systems," in Recent Advances in Refractory Alloys for Space Power Systems, pp. 1-18, NASA SP-245, (1970).

W.B. Pearson, A Handbook of Lattice Spacings and Structures of Metals and Alloys, Pergamon Press, New York (1958).

K.D. Sheffler, J.C. Sawyer, and E.A. Steigerwald, "Creep Behavior of Refractory Alloys in Ultrahigh Vacuum," in Recent Advances in Refractory Alloys for Space Power Systems, pp. 75-125, NASA SP-245, (1970).

J.R. Stephens, "Role of Hf and Zr in the Hydrogen Embrittlement of Ta and Cb Alloys," in Hydrogen in Metals, pp. 383-392, ASM, Metals Park, OH (1974).

J.R. Stephens, "Effects of Alloy Composition in Alleviating Embrittlement Problems Associated with the Tantalum Alloy T-111," NASA TN D-7838, (1975).

J.R. Stephens, "Effects of Long-Term Aging on Ductility of the Columbian Alloys C-103, Cb-1Zr, and Cb-75Z and the Molybdenum Alloy Mo-TZM," NASA TN-D-8095, (1975).

J.R. Stephens, "Effects of Long-Term Aging on Ductility and Microstructure of Cb and Mo Alloys," Metallography, 10, 1-25, (1977).

J.R. Stephens, "Effects of Alloy Composition in Alleviating Embrittlement Problems Associated with the Tantalum Alloy T-111," J. Less-Cmmon Metals, 51, 93-11, (1977).

G.K. Watson, J.R. Stephens, "Effect of Aging at 1040 °C (1900 °F) on the Ductility and Structure of a Tantalum Alloy, T-111," NASA TN-D-6988, (1972).

ORIGINAL PAGE IS
OF POOR QUALITY

TABLE 1. - COMPOSITION OF Ta, Nb, and Mo ALLOYS

Alloy	Ta	W	Mo	Hf	Nb	Zr	Ti	Re	C	H	N	O
	content, wt.%								content, ppm			
Ta-10W	Bal.	10.35	----	----	----	----	----	---	15	1.0	40	21
Ta-8W-0.5Hf		7.8	----	0.51	0.04	0.02	----	---	50	1.0	9	30
Ta-8W-1Re-0.7Hf-0.25 C (ASTAR 811 C)		7.5	----	.65	----	----	----	1.0	260	3.0	32	25
Ta-8W-1Hf		8.0	----	.9	0.04	0.03	----	---	50	1.6	5	24
Ta-8W-2Hf(T-111)		8.5	----	2.0	.05	.06	----	---	50	2.9	15	120
Ta-8W-3Hf		8.2	----	2.8	.04	.09	----	---	60	1.0	8	28
Ta-4W-2Hf		3.8	----	1.8	.04	.06	----	---	50	0.8	7	26
Ta-2Hf		-----	----	1.9	----	----	----	---	22	1.0	39	33
Nb-9.8Hf - 0.5Zr-1Ti 0.4Ta-0.4W (C-103)	0.4	0.4	----	9.8	Bal.	.52	0.95	---	<30	<5	40	130
Nb-10W-1Zr (Cb-752)	<0.05	9.8	----	<0.3	Bal.	<0.7	----	---	38	3	100	126
Nb-1Zr	-----	-----	----	---	Bal.	0.95	----	---	100	3	20	73
Mo-0.5Ti-0.1Zr (Mo-TZM)	-----	-----	Bal.	---	----	0.49	0.1	---	175	1	5	20

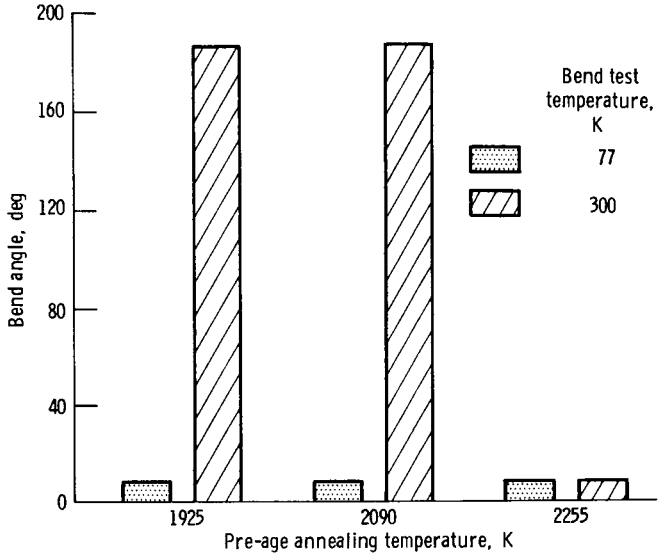

Figure 1. - Effect of pre-age annealing temperature on bend ductility of T-111 tube aged in lithium at 1315 K for 1000 hours.

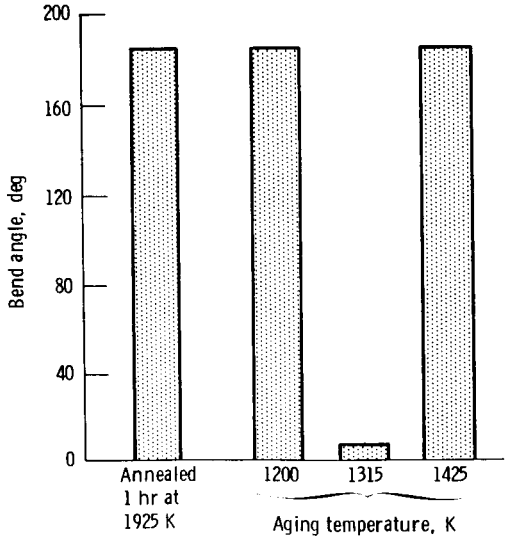

Figure 2. - Effect of aging temperature on bend ductility of T-111 tube aged in vacuum or lithium for 1000 hours.

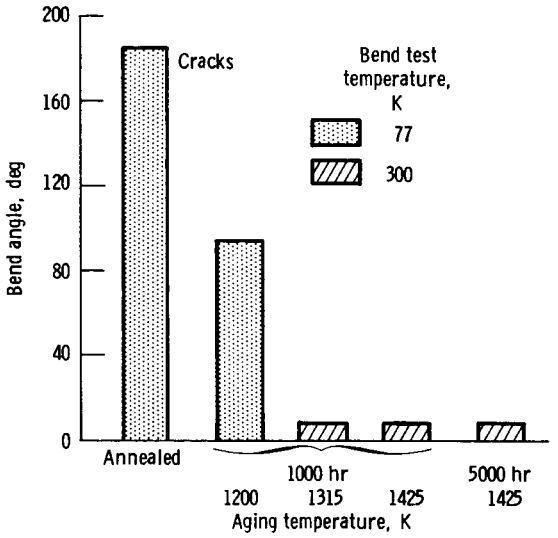

Figure 3. - Effect of hydrogen doping (10 ppm H) on bend ductility of T-111 sheet.

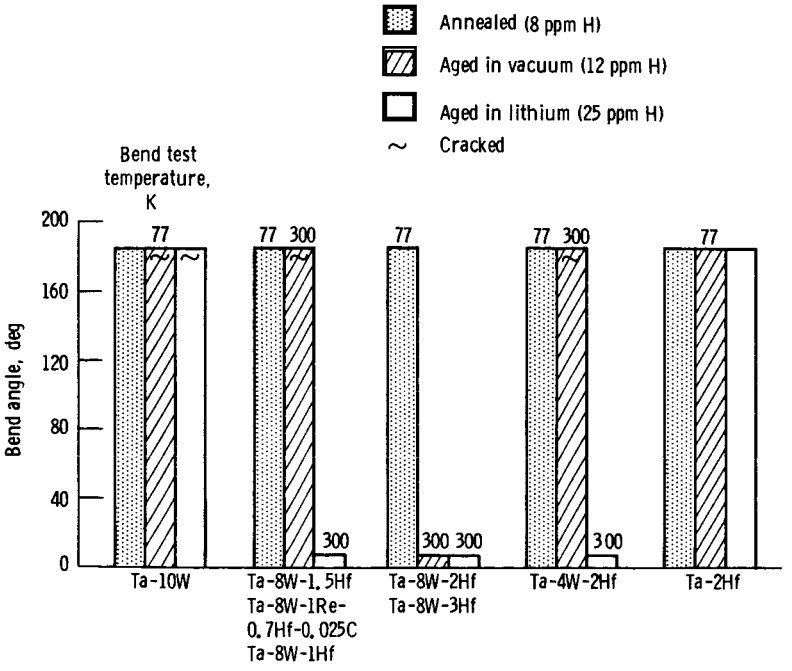

Figure 4. - Effect of hydrogen doping on bend ductility of annealed 1000 hour at 1315K and aged tantalum base alloys.

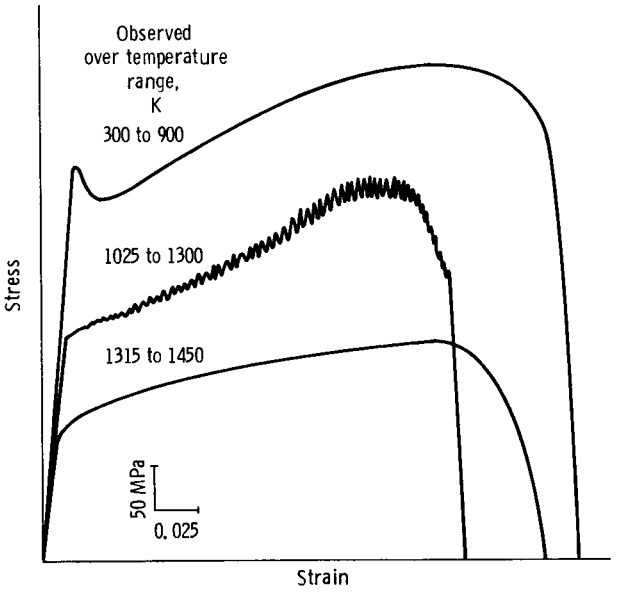

Figure 5. - Generalized engineering stress-strain curves for tantalum base alloys illustrating three types of flow behavior normally observed.

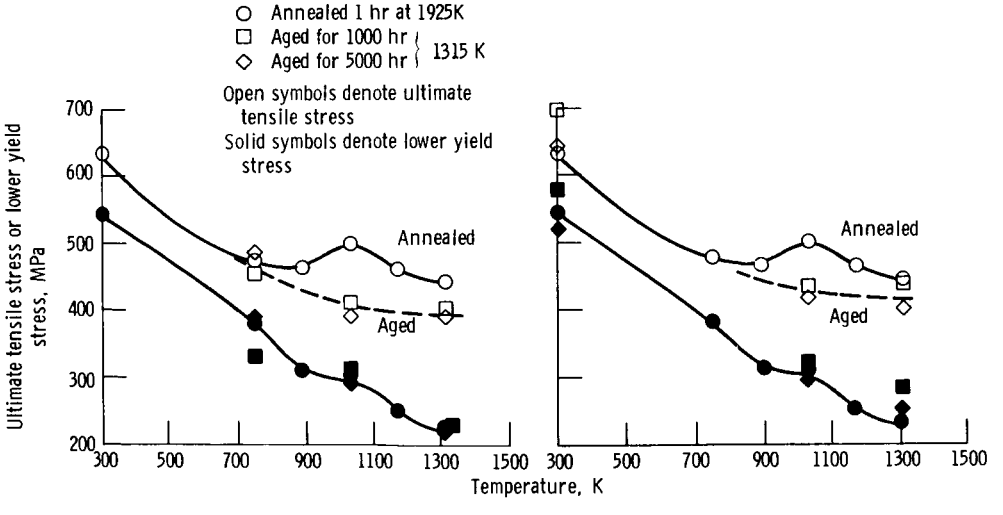

(a) Aged in vacuum.

(b) Aged in lithium.

Figure 6. - Effect of aging time at 1315K on ultimate tensile stress and lower yield stress of T-111 sheet.

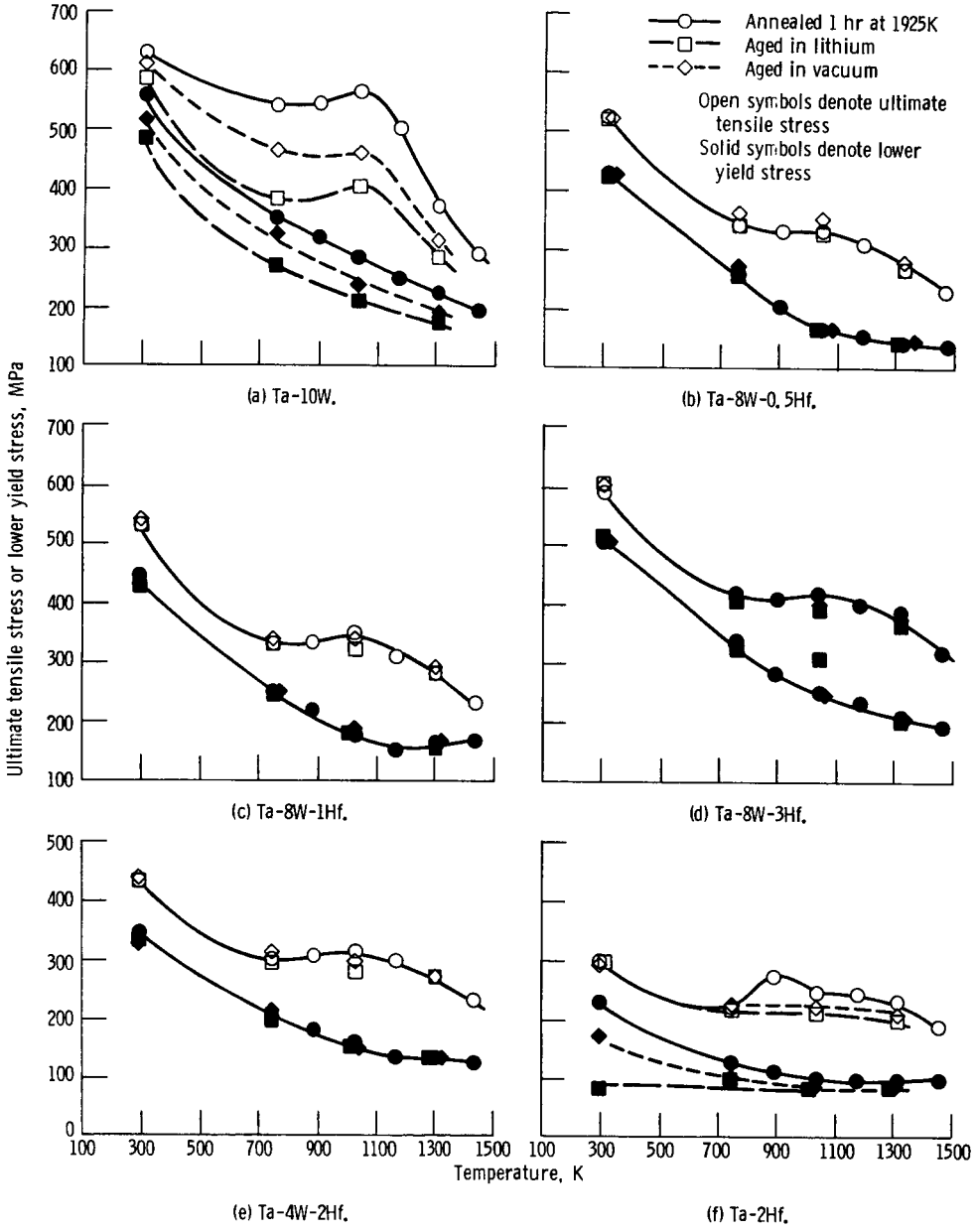

Figure 7. - Effect of aging 1000 hours at 1315K on ultimate tensile stress and lower yield stress of tantalum alloys.

ORIGINAL PAGE IS
OF POOR QUALITY

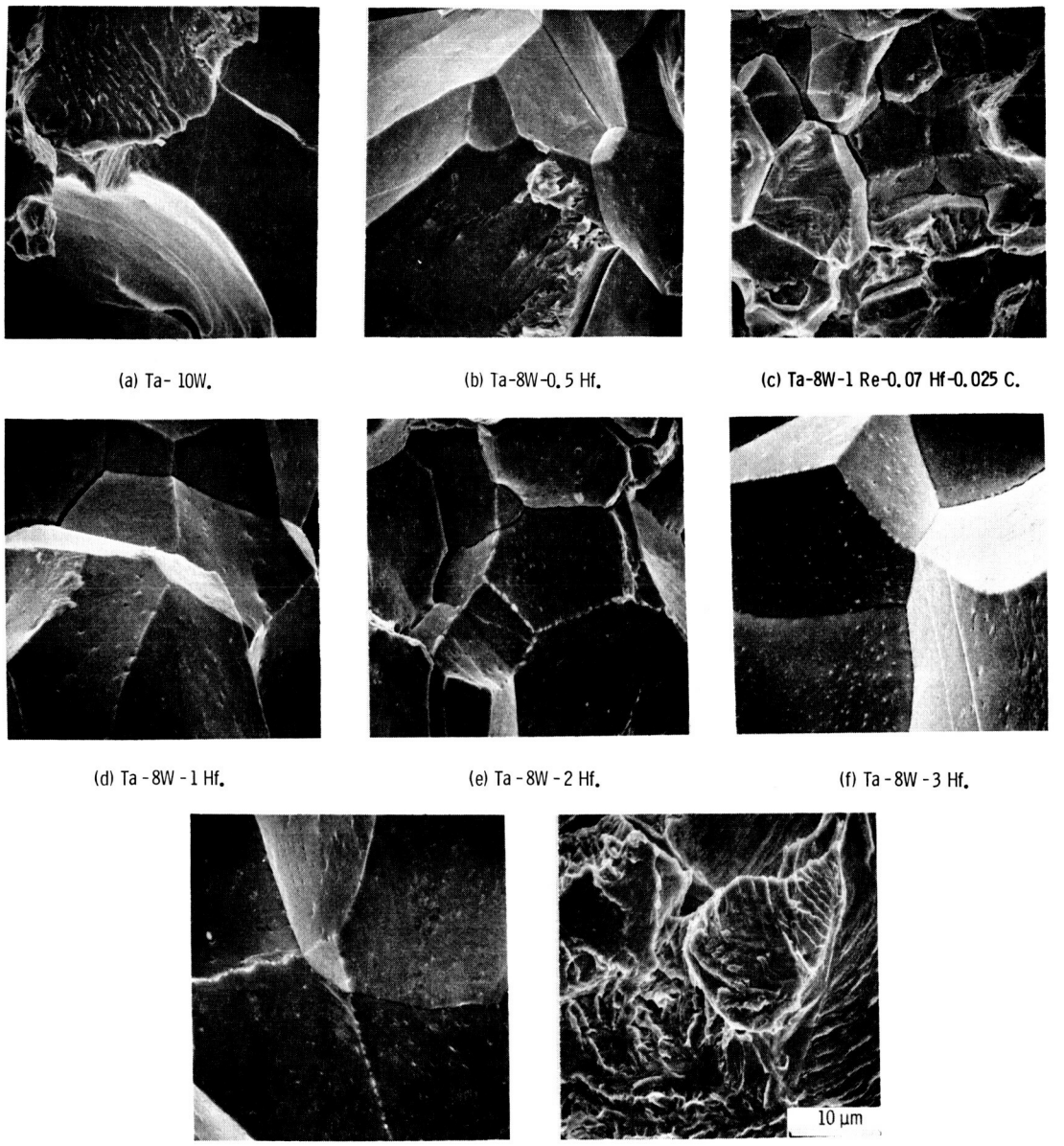

(a) Ta- 10W.

(b) Ta-8W-0.5 Hf.

(c) Ta-8W-1 Re-0.07 Hf-0.025 C.

(d) Ta - 8W - 1 Hf.

(e) Ta - 8W - 2 Hf.

(f) Ta - 8W - 3 Hf.

(g) Ta - 4W - 2 Hf.

(h) Ta - 2 Hf.

Figure 8. - Scanning electron micrograph of fractured surfaces of tantalum-base alloys aged 1000 hours at 1315 K. Hydrogen doped; bend tested temperature, 300 K.

ORIGINAL PAGE IS
OF POOR QUALITY

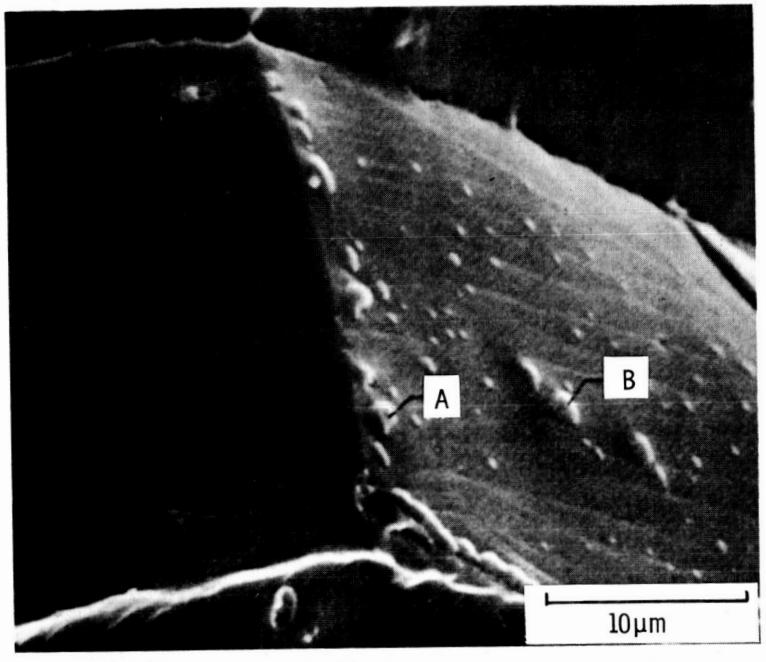

(a) Scanning electron micrograph.

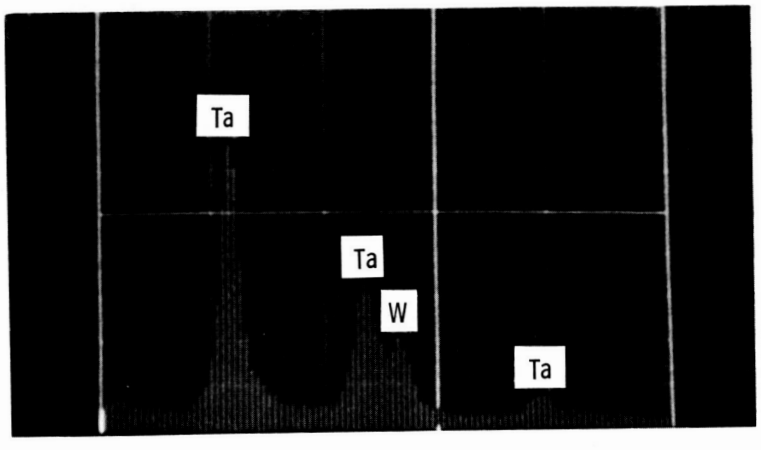

(b) Grain boundary surface.

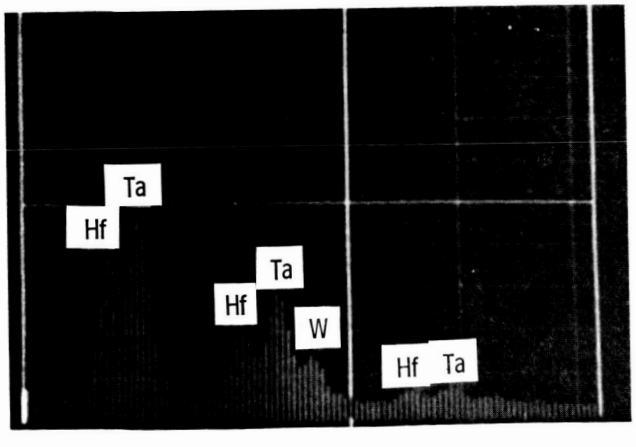

(c) Particle A.

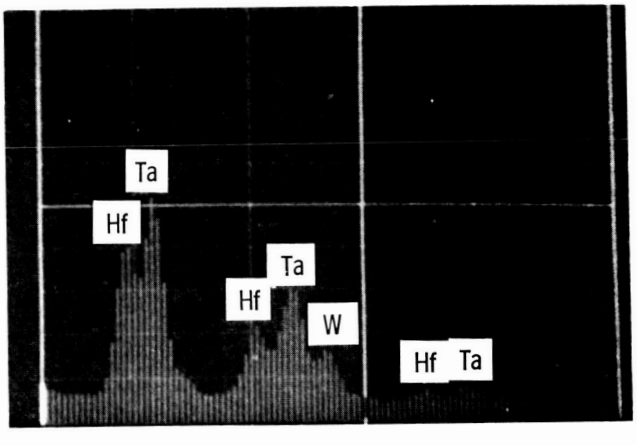

(d) Particle B.

Figure 9. - Scanning electron microscope analysis of precipitate particles observed in 1315 K aged T-111 sheet.

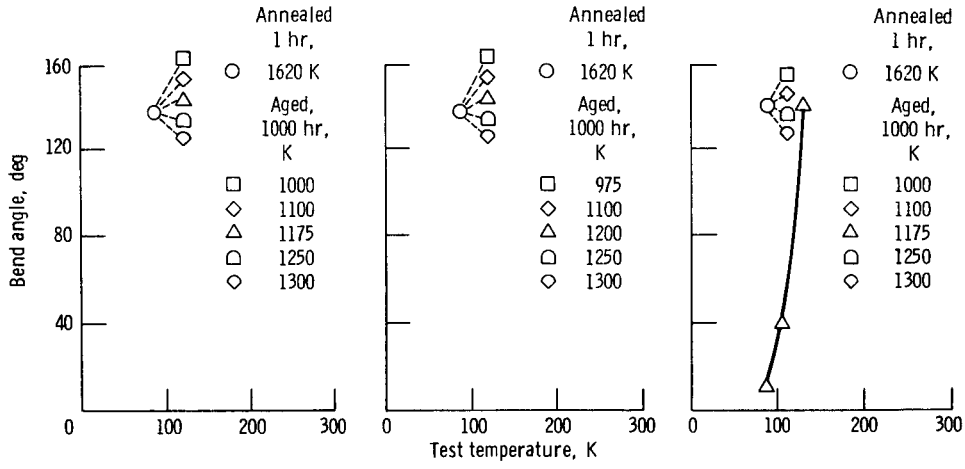

(a) C-103. (b) Nb-1Zr. (c) Cb-752.

Figure 10. - Effect of aging on the ductile-brittle transition temperature of niobium alloys.

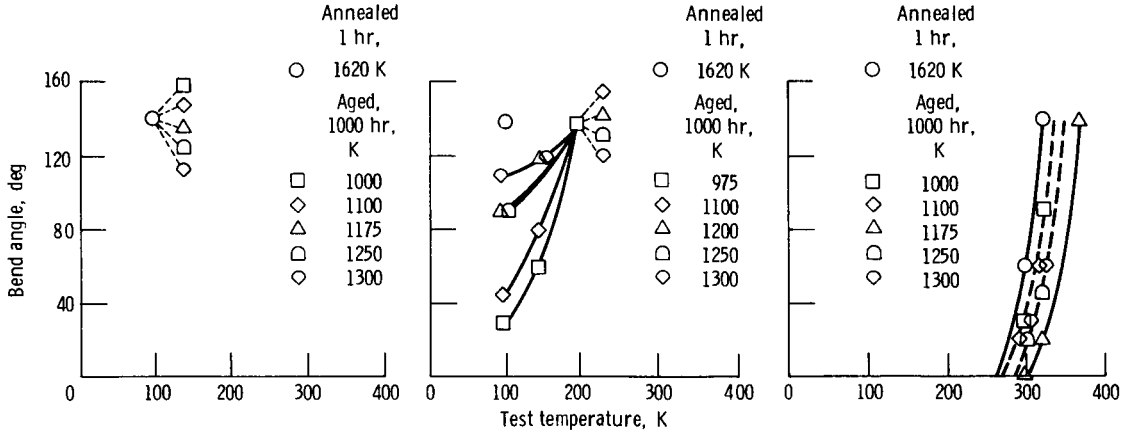

(a) C-103 + ~60 ppm H. (b) Nb-1Zr + ~50 ppm H. (c) Cb-752 + ~40 ppm H.

Figure 11. - Effect of hydrogen doping on the ductile-brittle transition ten perature of annealed and aged niobium alloys.

ORIGINAL PAGE IS
OF POOR QUALITY

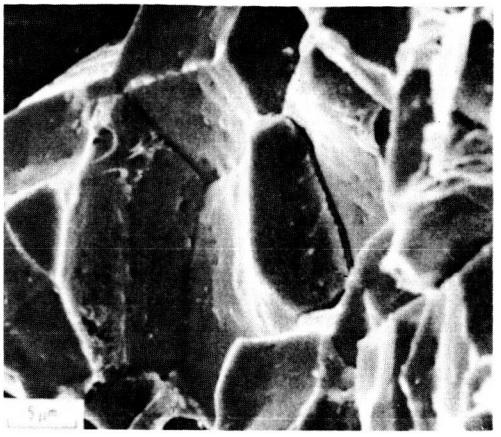

(a) Scanning electron micrograph.

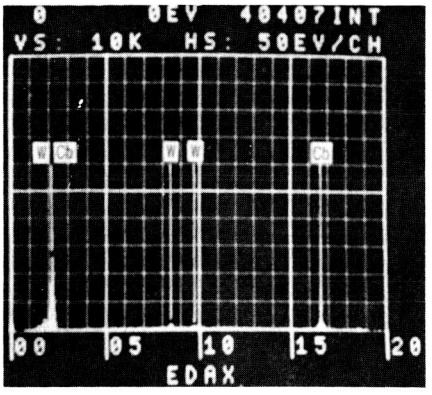

(b) Grain-boundary fracture surface analysis.

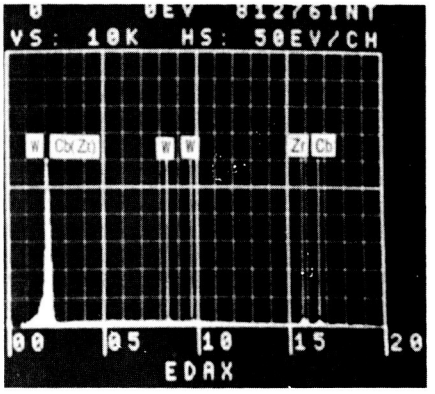

(c) Particle analysis.

Figure 12. - Scanning electron microscpoe analysis of fracture surface of 1175 K aged Cb-752. Test temperature 77 K.

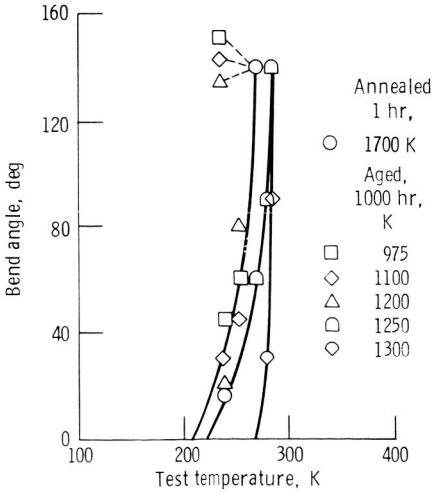

(d) Mo-TZM.

Figure 13. - Effect of aging on the ductile-brittle transition temperature of Mo-TZM.

ORIGINAL PAGE IS
OF POOR QUALITY

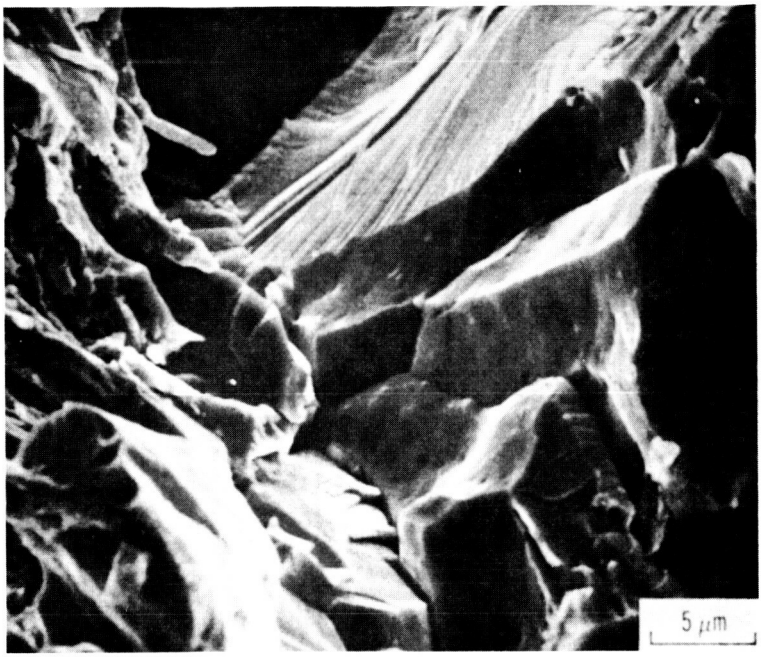

(a) Scanning electron micrograph.

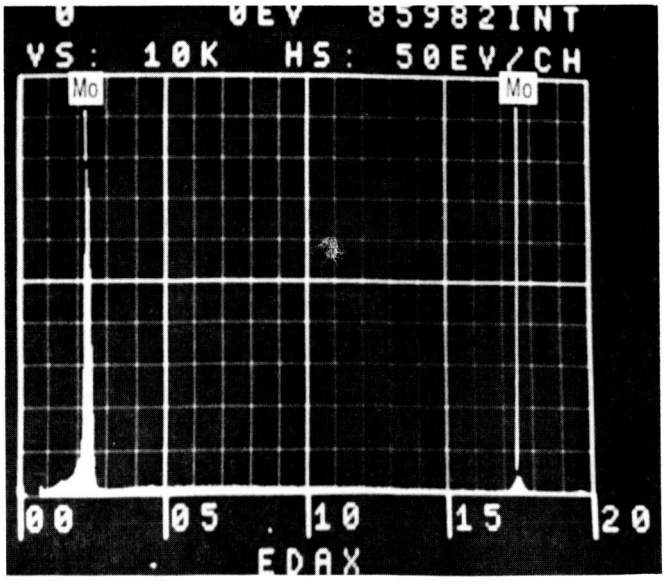

(b) Fracture surface analysis.

Figure 14. - Scanning electron microscope analysis of fracture surface of 1250 K aged Mo-TZM. Test temperature, 260 K.

1. Report No.	2. Government Accession No.	3. Recipient's Catalog No.
NASA TM-87210		

4. Title and Subtitle	5. Report Date
Thermal Aging Effects in Refractory Metal Alloys	
	6. Performing Organization Code: 505-63-01

7. Author(s)	8. Performing Organization Report No.
Joseph R. Stephens	E-2869
	10. Work Unit No.

9. Performing Organization Name and Address	11. Contract or Grant No.
National Aeronautics and Space Administration Lewis Research Center Cleveland, Ohio 44135	
	13. Type of Report and Period Covered: Technical Memorandum

12. Sponsoring Agency Name and Address	14. Sponsoring Agency Code
National Aeronautics and Space Administration Washington, D.C. 20546	

15. Supplementary Notes

Prepared for the Third Symposium on Space Nuclear Power Systems, sponsored by The American Nuclear Society, Albuquerque, New Mexico, January 13-15, 1986.

16. Abstract

The alloys of niobium and tantalum are attractive from a strength and compatibility viewpoint for high operating temperatures required in materials for fuel cladding, liquid metal transfer, and heat pipe applications in space power systems that will supply from 100 kWe to multi-megawatts for advanced space systems. To meet the system requirements, operating temperatures ranging from 1100 to 1600 K have been proposed. Expected lives of these space power systems are from 7 to 10 yr. A program was conducted at NASA Lewis to determine the effects of long-term, high-temperature exposure on the microstructural stability of several commercial tantalum and niobium alloys. Variables studied in the investigation included alloy composition, pre-age annealing temperature, aging time, temperature, and environment (lithium or vacuum), welding, and hydrogen doping. Alloys were investigated by means of cryogenic bend tests and tensile tests. Results showed that the combination of tungsten and hafnium or zirconium found in commercial alloys such as T-111 and Cb-752 can lead to aging embrittlement and increased susceptibility to hydrogen embrittlement of ternary and more complex alloys. Modification of alloy composition helped to eliminate the embrittlement problem.

17. Key Words (Suggested by Author(s))	18. Distribution Statement
Aging embrittlement; Hydrogen embrittlement; Tantalum; Niohium; Molybdenum; Lithium; Alloys	Unclassified - unlimited STAR Category 26

19. Security Classif. (of this report)	20. Security Classif. (of this page)	21. No. of pages	22. Price*
Unclassified	Unclassified		

*For sale by the National Technical Information Service, Springfield, Virginia 22161